FLASH SPECTROSCOPY OF PURPLE MEMBRANE

A. H. XIE,* J. F. NAGLE,* AND R. H. LOZIER‡
*Department of Physics, Carnegie-Mellon University, Pittsburgh, Pennsylvania 15213;
‡Cardiovascular Research Institute, University of California, San Francisco, California 94143

ABSTRACT Flash spectroscopy data were obtained for purple membrane fragments at pH 5, 7, and 9 for seven temperatures from 5° to 35°C, at the magic angle for actinic versus measuring beam polarizations, at fifteen wavelengths from 380 to 700 nm, and for about five decades of time from 1 μs to completion of the photocycle. Signal-to-noise ratios are as high as 500. Systematic errors involving beam geometries, light scattering, absorption flattening, photoselection, temperature fluctuations, partial dark adaptation of the sample, unwanted actinic effects, and cooperativity were eliminated, compensated for, or are shown to be irrelevant for the conclusions. Using nonlinear least squares techniques, all data at one temperature and one pH were fitted to sums of exponential decays, which is the form required if the system obeys conventional first-order kinetics. The rate constants obtained have well behaved Arrhenius plots. Analysis of the residual errors of the fitting shows that seven exponentials are required to fit the data to the accuracy of the noise level.

INTRODUCTION

Obtaining a model for the photocycle of bacteriorhodopsin (bR) in the purple membrane that is generally agreed upon by all workers has been a difficult task. It is generally agreed that there are at least four intermediates, named K, L, M and O, and that, relative to bR, M is strongly blue shifted, L is weakly blue shifted, and K and O are somewhat red shifted (Lozier et al., 1975). However, other intermediates have been suggested, including N (Lozier et al., 1975), P (Gillbro, 1978), X (Marcus and Lewis, 1978), and second M and L intermediates (Korenstein et al., 1978; Ohno et al., 1981). Furthermore, the pathways between intermediates have been disputed (Sherman et al., 1979; Beach and Fager, 1985), and the spectrum of the O intermediate is most poorly determined (Nagle et al., 1982).

All analyses of the photocycle must, at some early point, decide upon the number of intermediates in the photocycle. A systematic way to approach this is to fit the absorbance change data, $\Delta A(\lambda,t)$, to sums of exponential functions, i.e.,

$$\Delta A(\lambda,t) = \Sigma_{i=1,NL}\, b_i(\lambda) \exp(-k_i t), \qquad (1)$$

where the k_i are the apparent (i.e., observable) rate constants. According to a theorem in first-order kinetics, the precise number, NL, of exponential functions (including functions such as $t \exp[-kt]$ when accidental degeneracies occur in the rate constants) required to fit the data to within the statistical noise level is equal to the number of intermediates; this theorem is true for any such kinetic model regardless of the number of decay pathways and the corresponding number of true rate constants in the model. However, there are two important conditions that must hold for the theorem to pertain rigorously. The first condition for the theorem to apply is that the data obtained are indeed the true absorbance data unaltered by systematic errors. Considerable effort has been expended to ensure that this is the case and the precautions that we have taken will be discussed. The second condition is that the bR photocycle system does indeed obey first-order kinetics. The validity of this condition will be seriously questioned in the next paper where we consider the possibility of distributed kinetics, which changes the decay functions from exponentials to functions of another type. However, before attempting such refinements, it is important to establish carefully the number of intermediates, assuming that the simpler first-order kinetics pertain. This is the primary goal of this paper.

MATERIALS AND METHODS

Purple membrane samples were prepared from *Halobacterium halobium* strain JW-3 (ET1001) as described by Oesterhelt and Stoeckenius (1974), and then stored at −80°C in a density of ~2 mg purple membrane/ml in 45% sucrose (wt/wt). For the flash experiments ~5 mg of sample was repeatedly washed with distilled water, centrifuged, and decanted, resulting in a final sucrose concentration of <0.01% (wt/wt). The optical density (OD) of the samples was adjusted to be ~0.33 and the concentration of bR protein was 5.3 μmol. The samples were buffered to pH 5, 7, or 9 with a buffer consisting of 1 mM sodium acetate, 1 mM sodium phosphate, and 1 mM boric acid. The sodium concentration was 10 mM obtained from 7 mM NaCl in addition to the buffer. Each 3-ml sample was placed in a 1 × 1 × 4-cm optical cuvette for the flash experiment.

Our flash spectroscopy apparatus is sketched in Fig. 1. Many of the details of this apparatus have been discussed previously (Lozier, 1982) so we focus upon changes that have been made; some of the rationale for making these changes will be mentioned in the section on systematic errors. One change is that the measuring beam is now parallel to the actinic beam. Another change is the automatic taking of data at equal

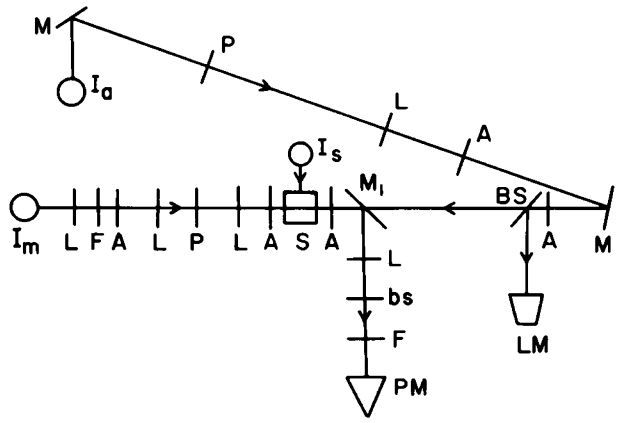

FIGURE 1 The optical arrangement of the apparatus. I_a is the actinic flash, I_m is the measuring beam with variable λ, and I_s is the side illumination. M, mirrors; BS, beam splitter; L, lenses; A, apertures; P, polarizers; F, filters; PM, photomultiplier; S, sample; bs, black spot; and LM, light meter. Mirror M_1 has a small aperature that passes the actinic beam. The black spot blocks the reflection of the laser beam from the cuvette.

intervals as a function of log time, rather than at equal intervals as a function of time. As has been discussed (Nagle, 1981), use of such a logarithmic time base is the only way that each decade of time has the same number of data points and that each decay rate is weighted impartially. Approximately 10 data points are taken in each decade of time from 1 μs to ~100 ms, where the latter time is adjusted for different temperatures according to the time required to complete the photocycle. Temperature control of the sample has been improved so that the temperature remains constant to within 0.02°C. An additional lamp filtered to transmit light at 500 ± 20 nm has been added to the system to provide side illumination to guarantee that the sample remains light adapted. The intensity of the side illumination on the sample was increased with increasing temperature; at

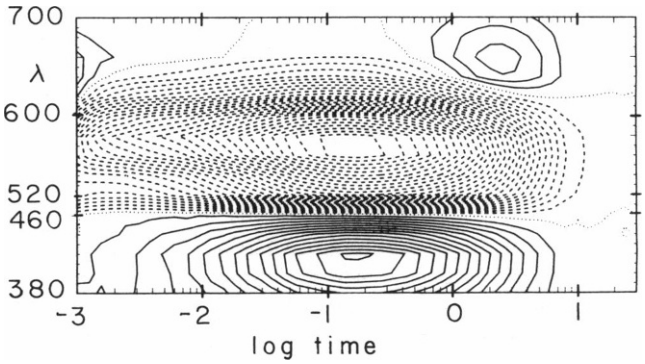

FIGURE 2 Contour plot of the absorbance changes, $\Delta A(\lambda,t)$, for a sample of purple membrane fragments in buffer at pH 7 and T = 30°C. Each contour denotes an increment of 2.0 milli OD with solid lines for positive ΔA, dashed lines for negative ΔA, and dotted lines for $\Delta A = 0$. Before the flash the total absorbance of the sample at 570 nm is 322 milli OD. The logarithm of the time in milliseconds is given on the horizontal axis to base 10, so −3 is 1 μs and 0 is 1 ms. The vertical axis gives the measuring wavelength λ in nanometers. Because of interference from the actinic flash at 490 nm, no data were taken at 480 and 500 nm and the otherwise linear wave length scale is compressed between 460 and 520 nm. The values of $\Delta A(\lambda,t)$ were obtained by computing $\Delta A(\lambda,t) = \log_{10}[I(\lambda,0)/I(\lambda,t)]$, where $I(\lambda,0)$ is the intensity of light transmitted with no actinic flash and $I(\lambda,t)$ is the intensity of light transmitted at time t after the actinic flash.

30°C it was 1.6 mW/cm^2. In some of the later experiments the side illumination was synchronized to go off 400 ms before the actinic flash and to go on again after completion of the photocycle. For most of our data the actinic wavelength was 490 nm and in some later data it was changed to 580 nm. When the actinic wavelength was 490 nm, measuring wavelengths at 480 and 500 nm were subject to strong flash artifact noise at early times and were consequently not included in the data sets that otherwise included measuring wavelengths at every 20 nm from 380 to 700 nm. Reduction of actinic light intensity was achieved with neutral density filters.

Nonlinear least squares fitting of exponentials according to Eq. 1. was performed using the variable projection algorithm (Golub and Pereyra, 1973). We used a version of the program especially designed by R. J. Leveque to fit the data at all wavelengths simultaneously with the same apparent rate constants, which is a fundamental requirement of the system. Early time points in the data were weighted less heavily in the fitting because of greater noise in that part of the data. Error estimates for the k_i were obtained as previously discussed (Nagle et al., 1982), except that the 95% confidence limit is given by 1.95σ not by 1.65σ.

The purely statistical error σ is the standard deviation computed from repeated (six times) data sets taken under the same conditions and with laser intensity fluctuations compensated for. The value of σ obtained was 0.10 milli OD for most times and most wavelengths. The expected errors are larger for shorter times, due to the averaging over less data in the log time data collector. The errors are also larger as the measuring wavelength decreases towards the ultraviolet because the measuring beam has weaker intensity which, along with the accompanying intrinsic noise, must be amplified more strongly.

RESULTS

The principal data were taken at pH 5, 7, and 9, and at the magic angle of 54.7° between the polarizations of the actinic beam and the measuring beam. Data were taken at 10, 20, and 30°C at 20-nm measuring wavelength intervals from 380 to 700 nm except for 480 and 500 nm. Data were also taken at 5°, 15°, 25°, and 35°C at measuring wavelengths of 420, 540, 600, and 640 nm. A contour plot of the absorbance change, ΔA is shown in Fig. 2 as a function of both wavelength and log time for T = 30°C and pH 7. Our presentation will focus upon this data set, although some final results for all data sets will be given and any notable differences will be mentioned. The peak negative absorbance changes in Fig. 2 are ~54 milli OD and the peak positive absorbance changes are ~28 milli OD. For the data in Fig. 2 the signal-to-noise ratio exceeds 500 for the maximum signals.

The results for the apparent rate constants, k_i, obtained from nonlinear least squares fitting are given in Table I for NL = 2 through 7 exponentials. Also shown in Table I are the corresponding amplitudes, $b_i(\lambda)$, for only four selected wavelengths, 420, 540, 600, and 660 nm. The goodness of the fits is indicated in Fig. 3 by contour plots of the residuals, $R(\lambda,t)$, which are just the differences between the actual data and the fitted values calculated from Eq. 1 using the parameters in Table I.

The data in Fig. 2 clearly require at least two exponentials because the absorbance change at most wavelengths proceeds from small absolute values at short times to much larger absolute values and then back to zero after the cycle is completed. However, this procession does not take place

TABLE I
RATE CONSTANTS AND SELECTED AMPLITUDES

			$b_i(\lambda)$			
NL	*i*	k_i	420	540	600	660
				λ		
2	2	25.2	−27.0	38.5	22.4	−0.4
	3	0.33	29.3	−48.9	−43.3	0.7
3	2	25.4	−29.3	34.5	25.8	6.6
	4	0.60	13.4	18.9	−19.8	−38.1
	3	0.33	17.5	−65.2	−25.8	34.0
4	1	795.0	−5.8	2.2	31.4	5.8
	2	23.1	−28.6	34.4	22.5	5.9
	4	0.60	15.2	14.5	−20.4	−36.6
	3	0.32	16.0	−61.4	−25.2	32.5
5	1	1,015.0	−5.5	−0.6	36.1	10.3
	2	32.8	−19.9	25.1	18.9	1.0
	5	10.3	−10.8	11.6	5.8	5.7
	4	0.69	16.9	6.1	−19.7	−32.0
	3	0.31	15.8	−54.2	−26.4	26.6
6	1	1,180.0	−5.4	−1.5	41.1	10.5
	2	46.2	−11.2	13.5	13.0	2.5
	5	16.0	−18.7	23.4	11.9	1.2
	7	3.5	−1.7	−1.3	1.5	7.0
	4	0.80	15.0	8.9	−17.6	−34.1
	3	0.31	18.2	−55.7	−29.3	25.2
7	1	1,163.0	−5.4	−1.5	40.6	10.4
	2	43.8	−12.8	15.6	14.0	2.6
	5	14.4	−18.0	22.3	11.4	1.3
	7	3.0	0.0	−3.8	−0.2	8.0
	4	0.79	11.9	17.6	−12.9	−40.4
	3	0.35	20.2	−61.5	−32.5	30.1
	6	0.05	0.4	−1.4	−0.6	0.2

Nonlinear least squares values of the apparent rate constants, k_i, and for the amplitudes, $b_i(\lambda)$, for λ = 420, 540, 600, and 660 nm only, for *NL* = 2–7, for the data in Fig. 2. The k_i are expressed in ms^{-1} and the $b_i(\lambda)$ in milli OD.

uniformly in time at all wavelengths, so that fitting with *NL* = 2 exponentials leaves a region, centered at 640 nm and 2 ms in Fig. 3 *a*, of very large (maximum of 8 milli OD) and correlated residuals. The term "large and correlated residuals" means that the residuals are large compared with the statistical noise level, $\sigma = 0.10$, and that they are correlated in that they have the same sign in a region; a region is defined to include several consecutive wavelengths and several consecutive times. The region of largest, correlated residuals in Fig. 3 *a* corresponds to a region of fairly small positive absorbance change in Fig. 2, which has been associated by many workers as the "O" intermediate, although it must be emphasized that one cannot make any quantitative predictions concerning the spectrum of "O" at this point in the analysis.

The existence of regions of large and correlated residuals is clear evidence that more exponentials are needed to fit the data. Proceeding to *NL* = 3 a new time constant near 2 ms is obtained and the region of large, correlated residuals is split into two regions of smaller residuals, and the residuals at all times later than 30 μs are also reduced, as seen in Fig. 3 *b*. The region of largest correlated residuals remaining in Fig. 3 *b* for *NL* = 3 is centered at 610 nm and 1 μs. (This feature is interpreted as the K intermediate by most workers.) Proceeding to *NL* = 4 exponentials reduces the residuals in this region and also for most times shorter than 1 ms, as seen in Fig. 3 *c*. The dramatic improvement in the fitting with the increase in the number of exponentials from 2 to 4 is consistent with the conclusion of numerous researchers that there are at least four intermediates in the photocycle for times later than 1 μs.

The naming convention of the apparent rate constants in Table I has the following, somewhat arbitrary, rationale. Roughly speaking, the larger *i* in k_i means that this rate constant is found "after" the preceding, lower numbered rate constants, where the "after" means that the nonlinear least squares fitting program obtains a better fit using the lower numbered rate constants when compared with replacing one of these by a higher numbered rate constant. This convention applies very nicely to k_3 and k_4 under all conditions studied. The convention obviously breaks down for widely separated rate constants, such as k_1 and k_3, especially when, as in Fig. 3, data are incomplete at early times when the k_1 decay is taking place. Therefore, in the case of k_1 the convention is supplemented by ordering the rate constants with smaller subscripts when they correspond to faster rates.

The conclusion that more than *NL* = 4 exponentials are required is apparent from Fig. 3 *c*. While the residuals are much smaller than in Fig. 3, *a* and *b*, nevertheless, there are regions of correlated residuals for the shorter times within which the residuals are more than seven times larger than the statistical noise σ. Proceeding to *NL* = 5 takes the single exponential with rate constant k_2 for *NL* = 4 in Table I and splits it into two exponentials. The name k_2 is retained for the faster one and the slower one has been called k_5 (Nagle et al., 1982). As seen in Fig. 3 *d* this results in substantial reduction of the residuals for times from 1 μs all the way to ~5 ms. However, there are still fairly large regions in which the residuals are correlated and have magnitudes greater than 3σ.

Proceeding to *NL* = 6, the next rate constant, called k_7, found in the nonlinear least squares fitting corresponds to a time constant, $1/k_7$, of 0.3 ms. As seen in Fig. 3 *e*, with the introduction of this exponential, the residuals become small and uncorrelated in the region consisting of the time domain from 10 to 5 ms and the wavelength domain from 440 to 700 nm. As mentioned in Materials and Methods, the residuals for the first decade of time from 1 to 10 μs and also in the blue region of wavelengths, 380–420 nm, are subject to greater noise than $\sigma = 0.1$. Therefore, the fit of Eq. 1 to the data can be considered satisfactory for all wavelengths and all times <4 ms.

Proceeding to *NL* = 7, another exponential with rate constant k_6 is obtained, which reduces all the residuals at

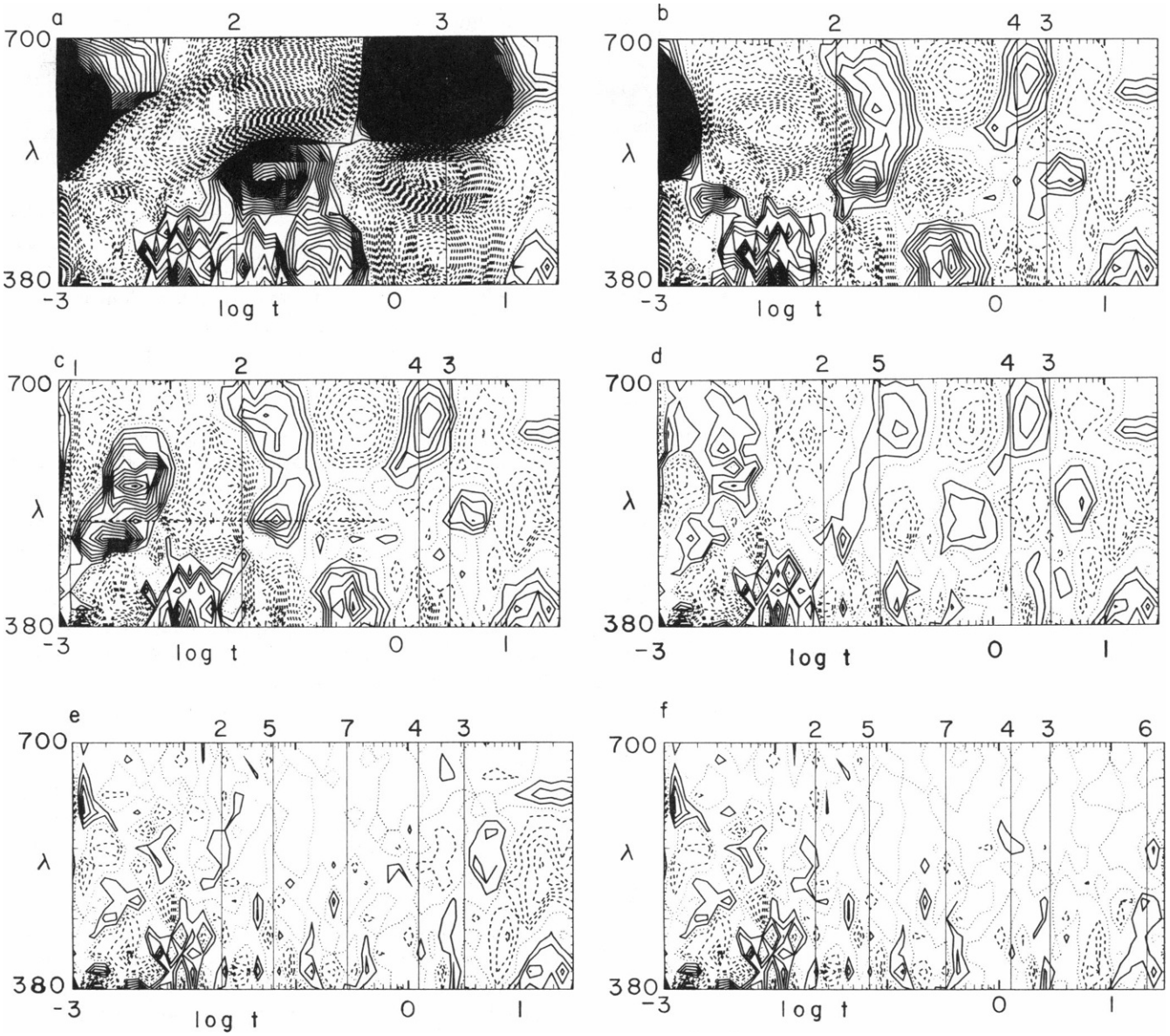

FIGURE 3 Contour plots of the residuals, $R(\lambda,t)$, obtained from the nonlinear least squares fitting to the data in Fig. 2. Each residual at each wavelength and time is the difference between the measured ΔA and the value computed from Eq. 1 with the parameters given in Table I. Each contour represents an increment of 0.1 milli OD in the residuals; 0.1 milli OD equals the statistical noise σ. The wavelength and log time scales are indentical to those in Fig. 2. Each solid vertical line gives the time constant, $1/k_i$, where the k_i are given in Table I for each value of NL and the value of i is shown at the top of the figure. k_i lies to the left of the figure for $NL > 4$. (*a*) $NL = 2$, $\sigma' = 1.95$ where σ' is the average error of the fit (Nagle et al., 1982); (*b*) $NL = 3$, $\sigma' = 0.58$; (*c*) $NL = 4$, $\sigma' = 0.30$; (*d*) $NL = 5$, $\sigma' = 0.19$; (*e*) $NL = 6$, $\sigma' = 0.15$; and (*f*) $NL = 7$, $\sigma' = 0.11$.

the longest times so that they are comparable to σ and/or uncorrelated over regions consisting of more than a few data points, as seen in Fig. 3 *f*. Regarding the naming of the last two rate constants, it may be noted that in some other data sets k_6 is found before k_7; also a very slow rate constant in the k_6 region has been found before (Gillbro, 1978) and was named k_6 (Nagle et al., 1982), whereas the rate constant that is called k_7 has been found for the first time in this study. The estimated uncorrelated errors for the k_i for $NL = 7$ and the pH 7, $T = 30$°C data are found to be 5% for k_1, 7% for k_2, 7% for k_5, 18% for k_7, 4% for k_4, 2% for k_3, and 23% for k_6. Even when correlations in the errors of two k_i are considered, the rate constants for $NL = 7$ remain well determined and separated from each other.

Upon proceeding to $NL = 8$, the nonlinear least squares program does not converge to a solution. This is a typical response when it is forced to try to fit too many exponentials to data that require fewer exponentials.

Another kind of statistical indicator of the goodness of the fit involves the normalized time correlation functions defined by

$$TC(\lambda) = \Sigma_{i-2,N} R(\lambda,t_i)^* R(\lambda,t_{i-1})/\text{NORM}, \qquad (2)$$

where the normalization factor is chosen so that the

maximum value of TC equals 1 when all the residuals have identical values. These correlations should take on random signs as a function of λ when NL is large enough. When NL is too small these correlations tend to become positive with values that approach 1 when the fitting is very poor. Fig. 4 shows that for $NL = 4$ the normalized time correlations are as large as 0.8 for many wavelengths and uniformly positive except for λ = 460 nm, at which λ all signals are small and the signal-to-noise ratio is low. As NL is increased, the time correlations become smaller, but only for $NL = 7$ does the sign of the time correlations become random.

We have also studied wavelength correlations, which are defined similarly to Eq. 2 except that the time is held constant and the sum is over wavelengths. These lead to the same conclusions as the time correlations. Another way to emphasize that the $NL = 7$ fitting is statistically meaningful is that the amplitudes, $b_j(\lambda)$, are smooth functions of λ, as shown in Fig. 5.

Arrhenius plots for the rate constants are given in Fig. 6. These plots include results from the data taken at the other temperatures and pH values. In the case of pH 7 it appears in Fig. 6 *b* that k_7 and k_5 become degenerate near T = 10°C. As discussed previously (Nagle et al., 1982), the nonlinear least squares fitting program finds one fewer rate constant at temperatures near a degeneracy. In the case of pH 5 and T = 5°C it appears that k_7 becomes nearly degenerate with k_4 and also k_6 becomes nearly degenerate with k_3, so an adequate fit is obtained with $NL = 5$. Similar degeneracies appear for pH 9 in Fig. 6 *c* at low temperatures. For temperatures 5°, 15°, 25°, and 35°C data were only taken at four wavelengths, 420, 540, 600, and 660 nm. This accounts for the slight oscillation that can be noticed in the values of k_6 in Fig. 6 *a* as a function of temperature at pH 5. Within statistical errors, the Arrhenius plots give straight lines for each rate constant.

The principal data were also taken with the polarizations of the actinic beam and the measuring beam both parallel and perpendicular, as well as at the more fundamental magic angle, which are the focus of this paper. (Previous results from this laboratory for the other polarizations have been given by Lozier and Parodi [1984].) From the measured dichroic ratio and the formulae of Nagle et al. (1983), the signal has reached 43% of saturation. Using the quantum efficiency ratio of 0.3:0.7 reported by Becher and Ebrey (1977) and the ratio 1.9 for the extinctions of bR and K at 490 nm (Nagle et al., 1982), it is estimated that 19% of the bR monomers are photocycling in the data presented in Fig. 2.

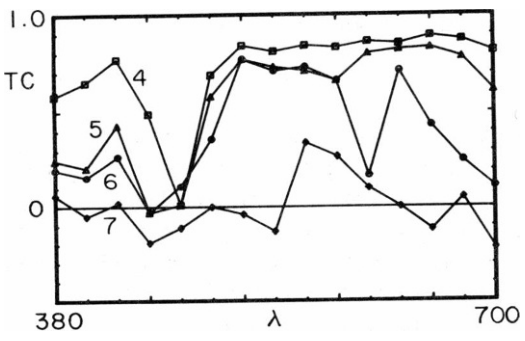

FIGURE 4 The time correlations defined in Eq. 2 as a function of λ for NL = 4, 5, 6, and 7 for the residuals shown in Fig. 3.

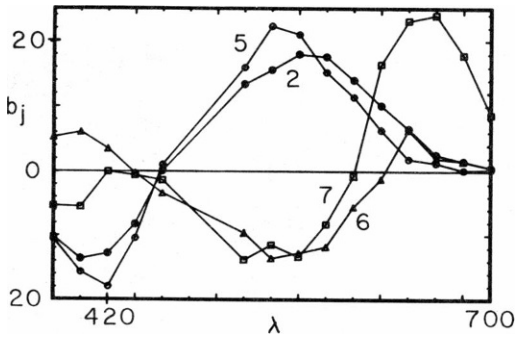

FIGURE 5 Some of the amplitudes, $b_j(\lambda)$, as a function of wavelength in nanometers for the $NL = 7$ fit. The amplitudes of b_6 are multiplied by 10 and the amplitudes of b_7 are multiplied by 3. For 480 and 500 nm the curves are interpolated from the 460 and 520 nm results. For clarity, amplitudes b_1, b_3, and b_4, which are very smooth functions of wavelength, are not shown. The reader is cautioned that the amplitudes are related to the spectra of the intermediates only in a rather complex way that is determined by the correct kinetic model.

Data were also taken at 20°C and pH 7 with the actinic wavelength at 580 nm and with a substantially lower actinic intensity so that the photocycling signal was only ~23% as large as for the previous, principal data. To achieve a comparable signal-to-noise ratio, these data required averaging over as many as 1,600 flashes for some measuring wavelengths compared with 80 flashes in the principal data. Measuring wavelengths were taken to be the same as previously except that no data were taken at 580 nm because of excessive flash artifact. Seven exponentials were again required to reduce the residuals to the noise level and to make the signs of the correlations random. Also, the rate constants determined from these data agreed within error with the rate constants plotted in Fig. 6.

SEARCH FOR SYSTEMATIC ERRORS

As has been mentioned (Nagle et al., 1983), Beer's law and the usual calculation of the absorbances from the logarithm of the transmitted intensities does not hold when the measuring beam crosses the actinic beam at right angles. Although the correction would appear to be <1% for samples with OD <0.5, the present configuration shown in Fig. 1 completely avoids this particular systematic error.

It is known that samples consisting of dispersions of large objects, such as cells or membranes, can have apparent spectra that differ from the true spectra of the homogenized solution because of the absorption flattening artifact (Duysens, 1956). Because the magnitude of the true positive absorption changes is decreased relative to the

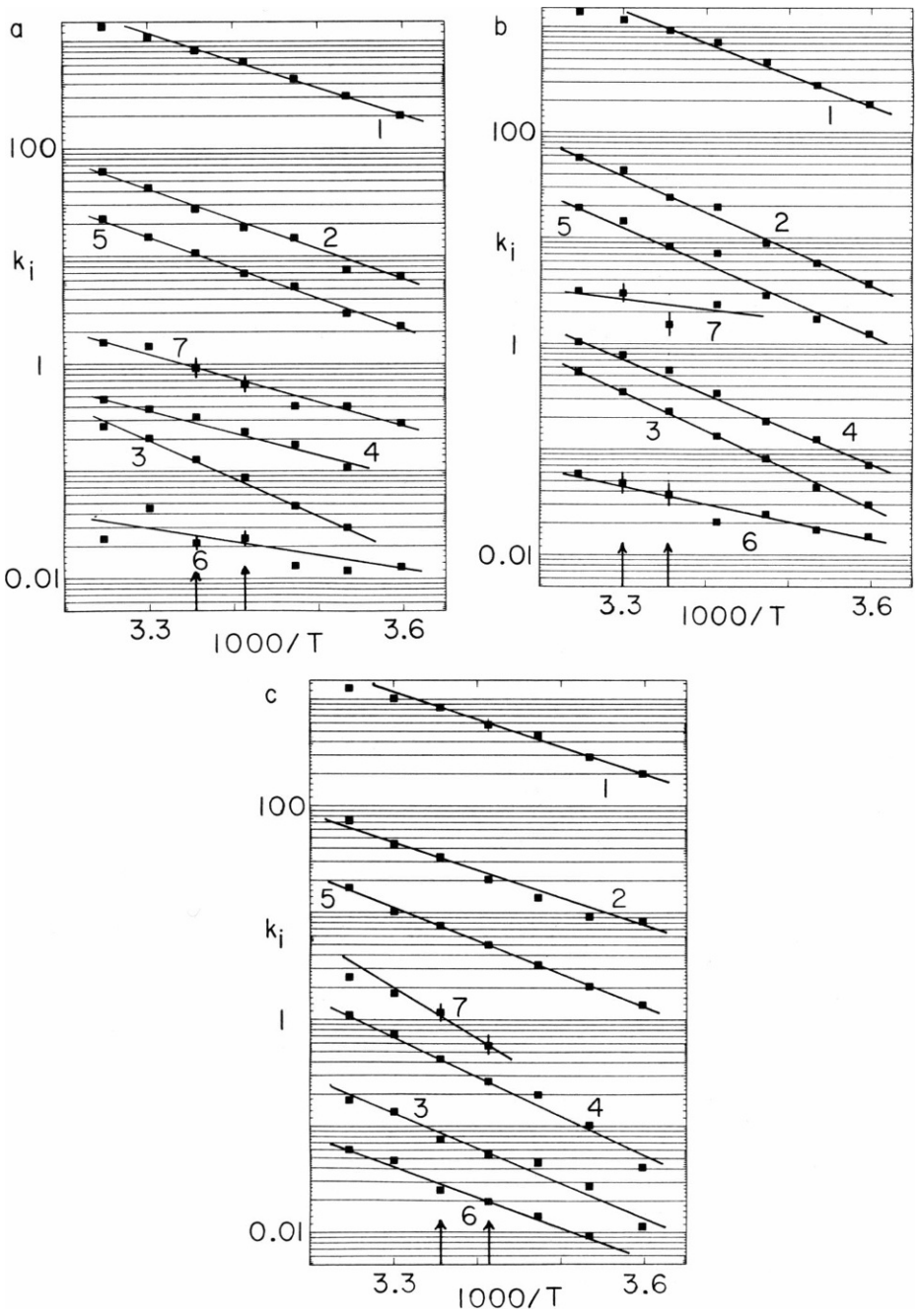

FIGURE 6 Arrhenius plots of the rate constants k_i in ms^{-1} for $i = 1$–7 for (*a*) pH 5, (*b*) pH 7, and (*c*) pH 9. For those selected temperatures indicated by vertical arrows on the horizontal axes error bars representing correlated errors are shown only for those rate constants whose errors exceed the size of the solid square symbol, indicating the value of the rate constant. Uncorrelated errors are even smaller than the correlated errors shown here (Nagle et al., 1982).

magnitude of the true negative absorption changes, the apparent absorption change data require more exponentials for an adequate fit, as we have verified numerically for some computer-generated data. We have made estimates of the degree of absorption flattening that would be expected for purple membranes 0.25 μm^2 in size, with the conclusion that, for visible wavelengths, absorption flat tening would alter the true absorption <0.3%. This would alter ΔA only by about as much as σ for the largest signals and would suggest that this problem could be ignored. However, the preceding calculation ignores the possibility of aggregation of the membranes, which would increase the systematic error in rough proportion to the mean number of membranes in each aggregate. This could easily magnify this systematic error to the same order of magnitude as those residuals that support the increase of NL beyond 4.

Although there is no obvious way to determine a priori

how much absorption flattening is present in a given sample, there is an obvious procedure for dealing with the absorption flattening artifact empirically. We first correct the apparent absorption change data assuming the strength of the flattening. Then we repeat the statistical analysis with the "corrected" data. The whole process is then repeated for different strengths of the flattening. That strength that gives the best fit to the data with the smallest value of NL should be the best candidate for the true strength of absorption flattening of the sample. To carry out this procedure, we corrected for the data using a simple quadratic correction term,

$$A_{\text{apparent}} = A_{\text{true}} - cA_{\text{true}}^2. \quad (3)$$

After subtracting out the nonphotocycling bR absorbance, $A_{\text{bR,true}}$, one obtains

$$\Delta A_{\text{apparent}} = \Delta A_{\text{true}}\,(1 - 2cA_{\text{bR,true}}) - c\Delta A_{\text{true}}^2. \quad (4)$$

Only the quadratic term will introduce new, spurious exponential terms into the data, so it suffices, for the purposes of determining the true number of intermediates to add a correction, $c\Delta A_{\text{apparent}}^2$, to the data. The result of doing this for the pH 7, $T = 30$°C data was a continuous worsening of the fitting to the data, either for $NL = 4$, which is the "minimal" NL believed possible, or for $NL = 5$. Therefore, we conclude from this empirical test that absorption flattening is not playing the role of making NL appear larger than it truly is. Glaeser and Jap (1985) have also concluded that absorption flattening does not play a significant role for purple membrane samples, even in CD spectroscopy.

It has been indicated (Czege, J., K. Hofmann, and W. Stoeckenius, personal communications) that light scattering changes during the photocycle. Since scattering also reduces the amount of light transmitted to the photomultiplier, it clearly introduces a systematic error into absorption change data. If the transient light scattering were due simply to the different intermediate forms of bR having different scattering power, then this systematic error is of no importance for the determination of the number of exponentials NL and it has minimal importance for any additional analysis of the photocycle. This follows because absorption changes measured in our experiments are simply the sum of the true absorption of light and the scattering of light and both parts would have the same time dependence, so the only change in Eq. 1 involves the amplitudes, $b_j(\lambda)$. Any spectra calculated in later analyses are also just the sum of the true absorbance and the scattering. It has also been suggested by J. Czege (personal communication) that transient scattering may be due to a change in shape of the membranes. If so, the kinetics of the scattering, while following the photocycle, might not necessarily obey Eq. 1 due to complex hydrodynamic effects. However, the change in scattering is only ~0.1% for pH 6 at 320 nm for small scattering angles (J. Czege). Unfortunately, it has not been indicated how large the total scattering is compared with the absorption, but it is clear that it should decrease rapidly as wavelength increases. Therefore, if one or more of the exponentials that we obtain in our fitting is due to scattering, then the corresponding amplitudes should systematically decrease in magnitude with increasing wavelength. This is contrary to our findings for any of the seven exponentials, so we conclude that scattering is unlikely to be significantly complicating our analysis of the photocycle.

As has been discussed before (Nagle et al., 1982, 1983), photoselection considerations show that the true chemical photocycle, unperturbed by physical motions and reorientations of the chromophores, can only be obtained when the actinic beam polarization and the measuring beam polarization are at the magic angle, ΔA_{M}. However, our measurements of the absorption changes when the beam polarizations are both parallel, ΔA_{par}, and perpendicular, ΔA_{perp}, give another check for systematic errors. There is a very general theorem that requires

$$E = 3\Delta A_{\text{M}} - 2\Delta A_{\text{perp}} - \Delta A_{\text{par}} = 0. \quad (5)$$

We find that, within statistical error, the quantity E is indeed zero.

The state of the sample during the measurement has been of concern for two reasons. First, small temperature fluctuations will alter the temperature dependent decay rates. At best, if the temperature fluctuations are fast and random during the time course of taking each data point, then each data point represents averages, the mean of which is the data for the mean temperature. However, if the temperature fluctuations are slower, then the data taken at different wave lengths may correspond to different temperatures, and therefore have different rate constants. We have improved our temperature control to 0.02°C, which, given the temperature dependence of the rate constants presented in Fig. 6, restrains the thermal fluctuations in the rate constants to be <0.2%. This, in turn, is less than the purely statistical error of 2% found in our determination of the rate constants, so no better temperature control is warranted.

It is important that the data be taken in a way that does not excite several different photocycles because it is much more difficult to unravel several independent photocycles, each of which may have multiple intermediate states, from the data than just one photocycle. We were concerned that an actinic flash at 490 nm, which is on the low wavelength side of the main bR absorption band, might be partially exciting a weaker absorption band in the blue. The fact that the later data taken with actinic wavelength 580 nm gives essentially the same results indicates that there is no such effect.

Another potential source of multiple photocycles is that the sample might be in a heterogeneous state preceding the actinic flash. (In this regard it is useful to note that light adapted bR contains at least 99% all-trans retinal; Scherrer et al., 1987). There are two sources of heterogeneity in

the state of the bR sample that have been eliminated. In light of sufficiently low intensity bR spontaneously transforms to a dark adapted form, which has a different photocycle than the all-trans light adapted form. The illumination of the laser actinic flash and the measuring beam suffices to keep the sample fully light adapted at temperatures below 20°C, but we found that additional illumination is needed at higher temperatures. Therefore, an additional side illumination was added to the apparatus.

The second source of sample heterogeneity is the actinic effect of the measuring beam on the sample. If a substantial fraction of the sample were photocycling at the time of the flash, the absorption of light by one of the intermediates could also begin a different cycle with intermediates and rate constants not present in the original photocycle that starts with bR → K. This effect has been minimized in this laboratory by using a monochromatic measuring beam. (An alternative arrangement employed in some other laboratories is to use white light and to select the wave lengths desired for the absorbance change measurements, but this means that a larger fraction of the sample is photocycling before the actinic flash.) However, our addition of a constant side illumination required to maintain the light adapted state also adds an unwanted actinic effect. In our principal data the intensity of the side illumination was carefully chosen for each temperature to ensure that it would be strong enough to keep the sample light adapted, but weak enough so that only ~0.2% of the photocycles would start from an intermediate rather than from bR, which would affect the maximum absorbance change by at most 0.12 milli OD, which is comparable to our purely statistical error σ. A control experiment for the actinic effect of the side illumination was to take data with the side illumination off as well as on at the lower temperatures, at which the side illumination was not required to maintain the bR in the light adapted state. Any observed differences were too small and in the wrong regions to account for the nonrandom, statistically significant residuals in Fig. 3, *d–f*. Also, the amplitudes, $b_5(\lambda)$, corresponding to the rate constant k_5 are far too large to be due to such a small fraction of unwanted photocycles, as are the b_7 amplitudes. Only the b_6 amplitudes are small enough for unwanted photocycles to be a real possibility. Our later data were taken with the side illumination sychronized to be off before and during the photocycle. The only systematic observed difference is that the b_6 amplitudes were roughly 0.4 milli OD more negative at most wavelengths.

A third source of sample heterogeneity occurs only after the flash. If a significant fraction of the bR molecules is excited by the flash, then a fraction of the trimers will have two or three excited bR molecules. For our highest light intensity for which 19% of the bR molecules are estimated to be photocycling, of those photocycling 34% would be in trimers with one or two other monomers also photocycling. Monomers of bR in trimers, which have different numbers of excited bR molecules, could well have different rate constants, thereby giving rise to a mixture of photocycles. This is the cooperativity effect that has been invoked (Korenstein et al., 1979; Ohno et al, 1981) to explain some rather large nonlinear effects with actinic light intensity for measuring wavelengths near 420 nm. We were concerned that such an effect could be responsible for splitting the rate constant k_2 into k_2 and k_5 and/or for producing k_6 and k_7, which have relatively small amplitudes. While no evidence for cooperativity has been found in this laboratory in the past for measuring wavelengths near 420 nm, a control experiment at 20°C and 23% of the light intensity was performed. In this control experiment the percentage of photocycling molecules in trimers containing one or two other photocycling molecules was only ~9%, so any pattern of statistically significant, correlated residuals that is caused by cooperativity should have been decreased by a factor of nearly four. No such decrease was observed for any *NL* value. This means that effects that are nonlinear with light intensity, which could be a manifestation of cooperativity, were too small to influence our data at a statistically significant level. Therefore, the conclusion remains that seven exponentials are required to fit the data to within the statistical noise level.

DISCUSSION AND CONCLUSIONS

The rate constants k_1, k_2, k_3, and k_4 have been recognized for a long time. In our previous study (Nagle et al., 1982) our statistical tests indicated the possible necessity of the additional rate constant k_5 and the k_6 rate constant first found by Gillbro (1978). However, our understanding of a number of possible causes of systematic errors and our control over the statistical errors were not sufficient at that time for us to conclude with confidence that the additional k_5 exponential was necessary in Eq. 1, especially since its temperature dependence was rather erratic. Accordingly, most of our subsequent analysis of the problem used only the minimal set of four rate constants. In the present study the temperature dependence of the k_5 rate constant is much more systematic as shown in the Arrhenius plots in Fig. 6. (Incidentally, we emphasize again that apparent rate constants are not required to plot as straight lines on Arrhenius plots, but their temperature dependence should follow rather smooth curves, especially since any phase transitions in this temperature range are weak and broad [Tristram-Nagle et al., 1986].) Furthermore, statistical errors are under control in the present study and all sources of systematic error that have hitherto been proposed have been dealt with, so we now have confidence that our absorbance change data give the true signature of the photocycle. The straightforward analysis in the results

section unequivocally leads to the conclusion that exponentials with rate constants k_5, k_6, and the new k_7 are necessary to fit our data using Eq. 1.

As was mentioned in the Introduction, the necessity of using seven exponentials to fit the data does not necessarily imply that there are as many as seven true intermediates in the photocycle. In particular, if one or more of the decays proceeds via the so-called distributed kinetics, then the number of true intermediates may be fewer than seven. This possibility will be analyzed in detail in a subsequent paper. Also, it is not possible without a great deal of further analysis to make statements about the spectral properties of the intermediates or about which kinetic pathways exist and the values of the true rate constants between intermediates (Nagle et al., 1982; Parodi et al., 1984). Such analysis is the focus of our current research.

This research was supported by a National Institutes of Health program project grant GM-27057 and National Science Foundation grant DMR-8115979.

Received for publication 14 August 1986 and in final form 15 December 1986.

REFERENCES

Beach, J. M., and R. S. Fager. 1985. Evidence for branching in the photocycle of bacteriorhodopsin and concentration changes of late intermediate forms. *Photochem. Photobiol.* 41:557–562.

Becher, B., and T. G. Ebrey. 1977. The quantum efficiency for the photochemical conversion of the purple membrane protein. *Biophys. J.* 17:185–191.

Duysens, L. M. N. 1956. The flattening of the absorption spectrum of suspensions, as compared to that of solutions. *Biochim. Biophys. Acta.* 19:1–12.

Gillbro, T. 1978. Flash kinetic study of the last steps in the photo-induced reaction cycle of bacteriorhodopsin. *Biochim. Biophys. Acta.* 504:175–186.

Glaeser, R. M., and B. K. Jap. 1985. Absorption flattening in the CD spectra of small purple membrane fragments. *Biochemistry.* 24: 6398–6401.

Golub, G. H., and V. Pereyra. 1973. The differentiation of pseudoinverses and nonlinear least-square problems whose variables separate. *SIAM (Soc. Ind. Appl. Math.) J. Numerical Anal.* 10:413–432.

Korenstein, R., B. Hess, and D. Kuschmitz. 1978. Branching reactions in the photocycle of bacteriorhodopsin. *FEBS (Fed. Eur. Biochem. Soc.) Lett.* 93:266–270.

Korenstein, R., B. Hess, and M. Markus. 1979. Cooperativity in the photocycle of purple membrane of *Halobacterium halobium* with a mechanism of free energy transduction. *FEBS (Fed. Eur. Biochem. Soc.) Lett.* 102:155–161.

Lozier, R. H. 1982. Rapid kinetic optical absorbption spectroscopy of bacteriorhodopsin photocycles . *Methods Enzymol.* 88:133–162.

Lozier, R. H., R. A. Bogomolni, and W. Stoeckenius. 1975. Bacteriorhodopsin: a light-driven proton pump in *Halobacterium halobium*. *Biophys. J.* 15:955–962.

Lozier, R. H., and L. A. Parodi. 1984. Bacteriorhodopsin: photocycle and stoichiometry. *In* Information and Energy Transduction in Biological Membranes. C. L. Bolis and E. J. M. Helmreich, editors. Alan R. Liss, New York. 39–50.

Marcus, M., and A. Lewis. 1978. Resonance Raman spectroscopy of the retinylidene chromophore in bacteriorhodopsin. *Biochemistry.* 17: 4722–4735.

Nagle, J. F. 1981. Upon the optimal graphical representation of flash data from photochemical systems obeying first order kinetics. *Photochem. Photobiol.* 33:937–939.

Nagle, J. F., L. A. Parodi, and R. H. Lozier. 1982. Procedure for testing kinetic models of the photocycle of bacteriorhodopsin. *Biophys. J.* 38:161–174.

Nagle, J. F., S. M. Bhattacharjee, L. A. Parodi, and R. H. Lozier. 1983. Effect of photoselection upon saturation and the dichroic ratio in flash experiments upon effectively immobilized systems. *Photochem. Photobiol.* 38:331–339.

Oesterhelt D. and W. Stoeckenius. 1974. Biomembranes. *Methods Enzymol.* 31:667–678.

Ohno, K., Y. Takeuchi, and M. Yoshida. 1981. On the two forms of intermediate M of bacteriorhodopsin. *Photochem. Photobiol.* 33:573–578.

Parodi, L. A., R. H. Lozier, S. M. Bhattacharjee, and J. F. Nagle. 1984. Inclusion of a backreaction in kinetic models of the photocycle of bacteriorhodopsin. *Photochem. Photobiol.* 40:501–512.

Scherrer, P., M. K. Mathew, W. Sperling, and W. Stoeckinius. 1987. Isomer ratio in dark adapted bacteriorhodopsin. *In* Biophysical Studies of Retinal Proteins. T. G. Ebrey, H. Frauenfelder, B. Honig, and K. Nakanishi, editors. University of Illinois Press, Urbana-Champaign, IL. In press.

Sherman, W. V., R. R. Eicke, S. R. Stafford, and F. M. Wasacz. 1979. Branching in the bacteriorhodopsin photochemical cycle. *Photochem. Photobiol.* 30:727–729.

Tristram-Nagle, S., C. P. Yang, and J. F. Nagle. 1986. Thermodynamic studies of purple membrane. *Biochim. Biophys. Acta.* 854:58–66.